Sound radiation quantities arising from a resilient circular radiator (without former Sec. VII, and with new order for references)

Ronald M. Aarts[a] and Augustus J.E.M. Janssen
Philips Research Europe
HTC 36 (WO-02)
NL-5656AE Eindhoven
The Netherlands

(Dated: August 20, 2009)

Power series expansions in ka are derived for the pressure at the edge of a radiator, the reaction force on the radiator, and the total radiated power arising from a harmonically excited, resilient, flat, circular radiator of radius a in an infinite baffle. The velocity profiles on the radiator are either Stenzel functions $(1-(\sigma/a)^2)^n$ with σ the radial coordinate on the radiator, or linear combinations of Zernike functions $P_n(2(\sigma/a)^2-1)$ with P_n the Legendre polynomial of degree n. Both sets of functions give rise, via King's integral for the pressure, to integrals for the quantities of interest involving the product of two Bessel functions. These integrals have a power series expansion and allow an expression in terms of Bessel functions of the first kind and Struve functions. Consequently, many of the results in [Piston radiator: Some extensions of the theory, J. Acoust. Soc. Am. **65**(3), 1979] are generalized and treated in a unified manner. A foreseen application is for loudspeakers. The relation between the radiated power in the near-field on one hand and in the far-field on the other is highlighted.

PACS numbers: 43.38 Ar, 43.20 Bi, 43.20 Px, 43.40 At
Keywords: piston sound radiation, sound power, loudspeaker, reaction force

I. INTRODUCTION

The analytical theory of sound radiation for the case of a harmonically excited, circular piston in an infinite baffle is firmly established in the literature. There are chapters in text books[1–5], survey papers[6,7] and many research papers from older[8–13] and more recent[14–21] years devoted to this subject. A big effort has been made to find series or convenient integral expressions for the sound pressure at all field points on or in front of the disk and the baffle. The single integral approach, in which the pressure is expressed via Rayleigh's integral[2] or by other means as a single integral with bounded integration limits, occurs in Refs.10, 11, 13, 15 and is reviewed, with emphasis on numerical work, in Ref.16. The spherical-wave-expansion approach uses Gegenbauer's addition theorem[22] to express the pressure as a series of integrals involving spherical Bessel functions and Legendre polynomials and can be found in Refs.15, 18–20, 23. Furthermore, King's integral[9] is used in Refs.6, 12, 14, 17, 19 and this yields expressions for the pressure in the form of an infinite integral involving the product of two Bessel functions and an exponential factor. In order that this integral can be used conveniently for computations, it is often necessary to employ somewhat more advanced complex function theory. Finally, in Ref.24 series expansions following from Rayleigh's integral[2] are given for the on-disk pressure, and in Ref.19 King's integral is used to develop a double-series expansion for the on-disk pressure.

In the present paper, single-series expressions are developed for quantities associated with the pressure (rather than for the pressure in the field itself) from King's integral. The velocity profile on the radiator is allowed here to be non-uniform. A set of results of this type, for the reaction force and the total radiated power, was obtained by Greenspan[6]. Greenspan considers, what are called in the present paper, Stenzel functions[8] $s^{(n)}(\sigma)=(1-(\sigma/a)^2)^n$, $0\le\sigma\le a$ $(n=0,1,2)$, and (infinitely supported) Gaussians and establishes series expansions and closed-form expressions for the quantities just mentioned. These results were derived from King's integral in an ad hoc manner with an impressive amount of analytical skill.

Greenspan's results will be generalized to velocity profiles of the Stenzel type of arbitrary order n and of the Zernike[25] type, see below, and linear combinations of the latter. The acoustical quantities considered here are edge pressure, reaction force, total power and directivity. Zernike functions have the form $R^0_{2n}(\sigma/a)=P_n(2(\sigma/a)^2-1)$, with P_n the Legendre polynomial of degree n. Linear combinations of both Stenzel functions and Zernike functions can be used to approximate any radially symmetric velocity profile. In this respect Zernike functions are much more effective, in terms of the required number of coefficients and amplitudes of these, than the Stenzel functions. Zernike functions have been considered recently[21] by the authors with respect to their potential and efficacy for forward computation of the on-axis and far-field pressure from a non-uniform velocity profile on the piston in terms of its Zernike expansion coefficients. Here it has been very helpful that Zernike functions are orthogonal and that many velocity profiles have Zernike coefficients that can be found in analytical form, see Ref.21, Appendix A. Moreover, the inverse

[a] Ronald.M.Aarts@philips.com

problem of estimating a velocity profile in terms of its expansion coefficients from on-axis pressure data has been considered in Ref.21. Results for quantities related to the pressure that admit an analytical treatment via King's integral were, however, not presented in Ref.21. This is done in the present paper: for the quantities of interest it will be shown that King's integral yields an attractive power series expansion.

Stenzel functions, with half-integer rather than integer order n, have been considered recently by Mellow[19] in the context of King's integral for the pressure. In Ref.19 these Stenzel type functions have been used to expand a non-uniform velocity profile for the purpose of computing the pressure everywhere on the radiator. This leads via King's integral to certain double series expansions for the pressure on the radiator that are more complicated than what is obtained here for the pressure at the edge of the radiator.

The paper is organized as follows. In Sec. II the basic formulas and functions are presented, and the results of the paper are discussed globally. In Secs. III, IV, and V the formulas for the pressure at the edge, the reaction force, and the total power and directivity are presented and discussed. These formulas are given for the case that v is a general (integer-order) Stenzel function or a linear combination of Zernike functions. In Sec. VI it is briefly indicated how the power can be estimated from near-field on-axis pressure data via the inverse method developed in Ref.21. In Sec. VII the conclusions are presented. Finally, in Appendix A the required integrals are computed in the form of power series in ka, and in Appendix B the convergence properties of these series are discussed.

II. BASIC FORMULAS AND OVERVIEW

The radiated pressure is given by Rayleigh's integral[2,26] as

$$p(\underline{r},t) = \frac{i\rho_0 ck}{2\pi}\, e^{i\omega t} \int_S v(\underline{r}_s)\, \frac{e^{-ikr'}}{r'}\, dS\ , \qquad (1)$$

where ρ_0 is the density of the medium, c is the speed of sound in the medium, $k = \omega/c$ is the wave number and ω is the radial frequency of the vibrating surface S for which a disk of radius a in an infinite baffle is taken. Furthermore, $\underline{r}$ is a field point, $\underline{r}_s$ is a point on the disk S, $r' = |\underline{r} - \underline{r}_s|$ is the distance between $\underline{r}$ and $\underline{r}_s$, and $v(\underline{r}_s)$ is the normal component of a (not necessarily uniform) velocity profile; see Fig. 1 for the geometry and notations. The time variable t in $p(\underline{r},t)$ and the harmonic factor $\exp(i\omega t)$ in front of the integral in Eq. (1) will be omitted in the sequel. The average velocity on S is denoted by V_s, hence the volume velocity V is given by

$$V = \int_S v(\underline{r}_s)\, dS = \pi a^2 V_s \qquad (2)$$

(the definition of V is in agreement with Greenspan's definition and notation[6], Eq. (2); in the present paper only V_s will be used).

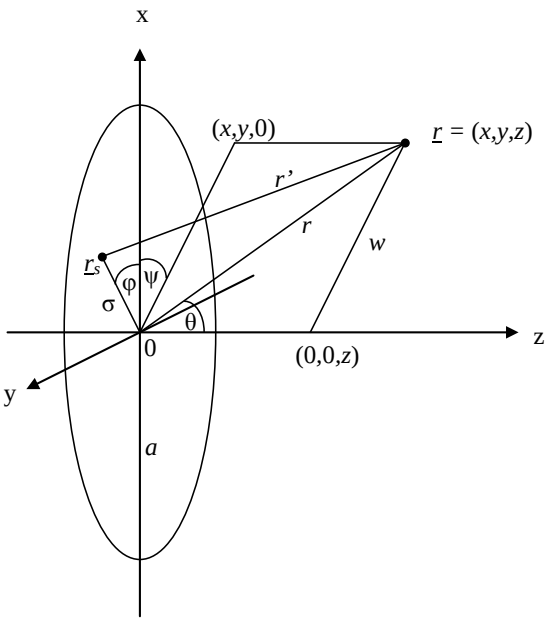

FIG. 1. Set-up and notations. The piston is surrounded by an infinite rigid baffle.

$$\begin{aligned}
\underline{r}_s &= (x_s, y_s, 0) = (\sigma\cos\varphi, \sigma\sin\varphi, 0)\\
\underline{r} &= (x,y,z) = (r\sin\theta\cos\psi, r\sin\theta\sin\psi, r\cos\theta)\\
w &= r\sin\theta = (x^2+y^2)^{1/2},\ \ z = r\cos\theta\\
r &= |\underline{r}| = (x^2+y^2+z^2)^{1/2} = (w^2+z^2)^{1/2}\\
r' &= |\underline{r} - \underline{r}_s| = (r^2+\sigma^2-2\sigma w\cos(\psi-\varphi))^{1/2}.
\end{aligned}$$

In the main body of this paper the velocity profile $v(\underline{r}_s)$ is assumed to be radially symmetric and is written as $v(\sigma)$, $0 \le \sigma \le a$ (with $v(\sigma) = 0$, $\sigma > a$). In the notations of Fig. 1, King's result[9] reads

$$\begin{aligned}
p(\underline{r}) &= \frac{i\rho_0 ck}{2\pi} \int_S v(\sigma)\, \frac{e^{-ikr'}}{r'}\, dS\\
&= i\rho_0 ck \int_0^\infty \frac{e^{-z(u^2-k^2)^{1/2}}}{(u^2-k^2)^{1/2}}\, J_0(wu)\, V(u)\, u\, du\ , \qquad (3)
\end{aligned}$$

where

$$(u^2-k^2)^{1/2} = \begin{cases} i\sqrt{k^2-u^2}\ , & 0 \le u \le k\ \ , \\ \sqrt{u^2-k^2}\ , & k \le u < \infty\ , \end{cases} \qquad (4)$$

with $\sqrt{\ }$ non-negative, and

$$V(u) = \int_0^a J_0(u\sigma)\, v(\sigma)\, \sigma\, d\sigma\ , \qquad u \ge 0\ , \qquad (5)$$

is the Hankel transform (of order 0) of v and $J_n(z)$ is the Bessel function of order n, where $n = 0$ in Eqs. (3) and (5).

In this paper two sets of functions for use in conjunction with King's result will be highlighted. The first set of functions are Stenzel's function $s^{(n)}(\sigma)$ given by

$$v(\sigma) = s^{(n)}(\sigma) = (n+1)V_s(1-(\sigma/a)^2)^n\ ,\ \ 0 \le \sigma \le a, \qquad (6)$$

with $n = 0, 1, \cdots$. To the authors' knowledge, Stenzel[8] was the first author to write on these functions in relation

to sound radiation (the profiles in Eq. (6) were considered extensively by Greenspan[6], but no reference to work of Stenzel can be found in Ref.6; also see Ref.7 (p.14)). The Hankel transform $S^{(n)}(u)$ of $s^{(n)}$ is given by[8]

$$S^{(n)}(u) = a^2(n+1)!\,2^n V_s \frac{J_{n+1}(au)}{(au)^{n+1}} \ . \tag{7}$$

A second set of functions considered in this paper are the Zernike functions

$$R^0_{2n}(\sigma/a) = P_n(2(\sigma/a)^2 - 1) \ , \ \ 0 \le \sigma \le a \ . \tag{8}$$

Any radially symmetric velocity profile $v(\sigma)$, $0 \le \sigma \le a$, allows an (orthogonal) expansion as

$$v(\sigma) = V_s \sum_{n=0}^{\infty} u_n R^0_{2n}(\sigma/a) \ , \tag{9}$$

where $u_0 = 1$ (this follows from the definition in Eq. (2) and the fact that $\int_0^a R^0_{2n}(\sigma/a)\sigma d\sigma = \frac{1}{2}a^2\delta_{n0}$). The Hankel transform $V(u)$ of $v(\sigma)$ in Eq. (9) is given by[21,25,27]

$$V(u) = V_s \sum_{n=0}^{\infty} u_n (-1)^n \frac{a}{u} J_{2n+1}(ua). \tag{10}$$

After inserting Eq. (7) or Eq. (10) into Eq. (3), integrals of the form

$$\int_0^{\infty} e^{-z(u^2-k^2)^{1/2}} \frac{J_\nu(wu)J_\mu(au)}{u^\lambda (u^2-k^2)^{1/2}} u du \tag{11}$$

with $\nu = 0$ appear. These integrals seem too complicated to allow a completely analytic treatment. However, there are cases with $z = 0$ and $w = a$ that allow such a treatment. These cases occur

a) for the pressure at the edge with $\underline{r} = (a\cos\psi, a\sin\psi, 0)$, and $w = a$, see Sec. III,

b) in the computation of the reaction force $F = \int_S p dS$ on the radiator, see Sec. IV,

c) in the computation of the radiated power $P = \int_S p v^* dS$, see Sec. V.

The quantity in a) was expressed in terms of Bessel and Struve functions by Warren[28] for the case $n = 0$, and this result was proved and generalized (to the cases $n = 0, 1$) by McLachlan[24]. The quantities mentioned in b) and c) were expressed by Rayleigh[26] (case b), $n = 0$) and Greenspan[6] (cases b) and c), $n = 0, 1, 2$) for the case of Stenzel radiators $s^{(n)}$ in terms of Bessel and Struve functions, and Greenspan gives the first few power series coefficients of reaction force and power as a function of ka. Moreover, Greenspan obtains similar results for the (infinitely supported) Gaussian. In the present paper the quantities in a), b) and c) will be computed as power series for all Stenzel cases $v = s^{(n)}$ and for all terms and cross terms pertaining to $v(\sigma)$ in Eq. (9). The coefficients of these power series are organized in such a way that the close connection between the integral expression on one hand and the Bessel functions of the first kind and the Struve functions on the other hand is immediately apparent. Finally, the series are cast into single-series format which makes them convenient to use. Greenspan's results have been used as a check of correctness of the formulas here. To facilitate this, the formulas have been brought into the same form as Greenspan's results. Also a number of cross-checks have been carried out.

The main results of this paper follow from the power series expansions in ka of the integrals that appear in Eq. (11) with $w = a$ and $z = 0$. These power series are derived in Appendix A. In Appendix B the convergence behavior of these expansions are considered. It thus appears that all series provide 10^{-6} absolute accuracy when they are truncated at a summation index $\ge 2eka{+}10$ and when $ka \le 12$ (machine precision 10^{-15}).

III. PRESSURE AT THE EDGE

According to Eq. (3), the pressure $p_{\rm edge}$ at an edge point $(a\cos\psi, a\sin\psi, 0)$ of the radiator is obtained by taking $z = 0$ and $w = a$. Thus

$$p_{\rm edge} = i\rho_0 ck \int_0^{\infty} \frac{J_0(au)V(u)}{(u^2-k^2)^{1/2}} u du \tag{12}$$

with $V(u)$ the Hankel transform in Eq. (5) of $v(\sigma)$.

A. Stenzel functions

With $v(\sigma) = s^{(n)}(\sigma)$, see Eq. (6), for which the Hankel transform $S^{(n)}(u)$ is given by Eq. (7), the pressure $p^{(n)}_{\rm edge}$ at the edge is given by

$$\frac{p^{(n)}_{\rm edge}}{\rho_0 c V_s} = \frac{ik(n+1)!2^n}{a^{n-1}} \int_0^{\infty} \frac{J_0(au)J_{n+1}(au)}{u^n(u^2-k^2)^{1/2}} du \ . \tag{13}$$

The integral in Eq. (13) has been evaluated in Appendix A.1 and the result is

$$\begin{aligned}
\frac{p^{(n)}_{\rm edge}}{\rho_0 c V_s} &= (n+1)!\Big(\frac{2}{a}\Big)^n ka\Big[\int_0^k \frac{J_0(au)J_{n+1}(au)}{u^n\sqrt{k^2-u^2}} du \\
&\quad + i\int_k^{\infty} \frac{J_0(au)J_{n+1}(au)}{u^n\sqrt{u^2-k^2}} du\Big] \\
&= \frac{1}{2}(n+1)!ka\Big[\sum_{j=0}^{\infty} \frac{(-1)^j(2j+2)_n(ka)^{2j+1}}{\Gamma^2(n+j+2)} \\
&\quad + i\sum_{j=0}^{\infty} \frac{(-1)^j(2j+1)_n(ka)^{2j}}{\Gamma^2(n+j+3/2)}\Big] \\
&= -\frac{1}{2}(n+1)!\sum_{\ell=1}^{\infty} \frac{(\ell)_n(-ika)^\ell}{\Gamma^2(n+\frac{1}{2}\ell+1)} \ .
\end{aligned} \tag{14}$$

Here Γ is the Gamma function and $(x)_n$ is Pochhammers's symbol as defined in Eq. (A13).

The middle expression for $p^{(n)}_{\rm edge}$ in Eq. (14) is convenient for expressing $\Re p^{(n)}_{\rm edge}$ and $\Im p^{(n)}_{\rm edge}$ in terms of Bessel functions of the first kind and Struve functions, respectively, see Eqs. (A4) and (A5). Thus for the case that

$n=0$, it is seen that (using $(x)_0=1$)

$$\frac{p^{(0)}_{\rm edge}}{\rho_0 c V_s}=\frac{1}{2}\Big[1-J_0(2ka)+i\mathbf{H}_0(2ka)\Big], \qquad (15)$$

a result given by Warren[28] (without proof) and proved and discussed by McLachlan[24]. For the case that $n=1$, the coefficients in the two series in the middle expression for $p^{(1)}_{\rm edge}$ in Eq. (14) must be manipulated. Thus one has (using $(x)_1=x$)

$$\sum_{j=0}^{\infty}\frac{(-1)^j(2j+2)z^{2j+1}}{\Gamma^2(j+3)}=2\frac{1-J_0(2z)}{z^3}-2\frac{J_1(2z)}{z^2}, \qquad (16)$$

$$\sum_{j=0}^{\infty}\frac{(-1)^j(2j+1)z^{2j}}{\Gamma^2(j+5/2)}=\frac{2}{z^3}\mathbf{H}_0(2z)-\frac{2}{z^2}(\frac{4}{\pi}-\mathbf{H}_1(2z)), \qquad (17)$$

where $\mathbf{H}_n(z)$ is the Struve function of order n, and with $z=ka$ it follows that

$$\frac{p^{(1)}_{\rm edge}}{\rho_0 c V_s}=2\Big\{\frac{1-J_0(2z)}{z^2}-\frac{J_1(2z)}{z}+ i\big[\frac{1}{z^2}\mathbf{H}_0(2z)-\frac{1}{z}(\frac{4}{\pi}-\mathbf{H}_1(2z))\big]\Big\}. \qquad (18)$$

This agrees with the result in Ref.24, Eq. (34), except for the overall factor 2 (due to the definition of $v^{(n)}$ in Eq. (6)) and the signs in front of $J_1(2z)/z$ and $\mathbf{H}_1(2z)$. Since $p^{(1)}_{\rm edge}\to 0$ as $k\to 0$, the correct signs are as in Eq. (18). In Fig. 2 $|p^{(n)}_{\rm edge}/\rho_0 c V_s|$ vs. ka is plotted (using the last formula of Eq. (14)) for the rigid piston ($n=0$), the simply supported radiator ($n=1$) and the first two clamped radiators ($n=2,3$).

It is observed that the coefficient of $(ka)^2$ in $p^{(n)}_{\rm edge}$ equals $\frac{1}{2}\rho_0 c V_s$ (independent of n). Thus $\Re[p^{(n)}_{\rm edge}]\approx\frac{1}{2}\rho_0 c V_s(ka)^2$ for small ka.

B. Zernike functions

With $v(\sigma)$ a linear combination of Zernike functions $R^0_{2n}(\sigma/a)$ as in Eq. (9), for which the Hankel transform $V(u)$ is given by Eq. (10), the pressure $p_{\rm edge}$ at the edge is given by

$$\frac{p_{\rm edge}}{\rho_0 c V_s}=ika\sum_{n=0}^{\infty}(-1)^n u_n\int_0^{\infty}\frac{J_0(au)J_{2n+1}(au)}{(u^2-k^2)^{1/2}}du\,. \qquad (19)$$

The integrals in Eq. (19) have been evaluated in Appendix A.2, with the result that

$$i\int_0^{\infty}\frac{J_0(au)J_{2n+1}(au)}{(u^2-k^2)^{1/2}}du=\int_0^{k}\frac{J_0(au)J_{2n+1}(au)}{\sqrt{k^2-u^2}}du + i\int_k^{\infty}\frac{J_0(au)J_{2n+1}(au)}{\sqrt{u^2-k^2}}du=$$

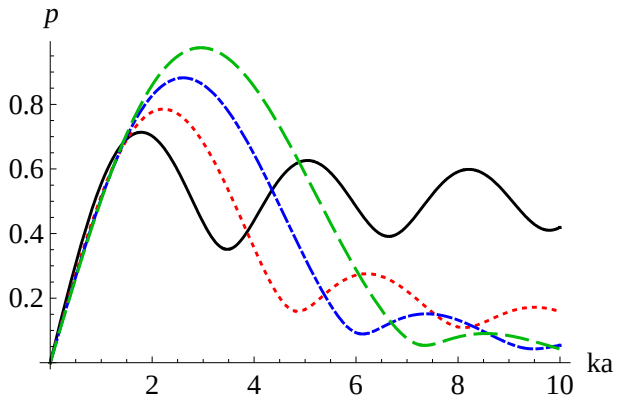

FIG. 2. (Color online) The pressure at the edge $|p^{(n)}_{\rm edge}/\rho_0 c V_s|$ vs. ka, for the rigid piston ($n=0$) (solid curve), the simply supported radiator ($n=1$) (dotted curve) and the first two clamped radiators ($n=2,3$) (dash-dotted and dashed curves, respectively).

$$\frac{1}{2}\sum_{j=0}^{\infty}(-1)^j\Big(\frac{(j+1)_n}{\Gamma(2n+j+2)}\Big)^2(ka)^{2n+2j+1}+$$

$$\frac{1}{2}i(-1)^n\sum_{j=0}^{\infty}(-1)^j\Big(\frac{(-j+1/2)_n}{\Gamma(j+n+3/2)}\Big)^2(ka)^{2j}$$

$$=\frac{-(-1)^n}{2ka}\sum_{\ell=1}^{\infty}\Big(\frac{(-\frac{1}{2}\ell+1)_n}{\Gamma(n+\frac{1}{2}\ell+1)}\Big)^2(-ika)^{\ell}\,. \qquad (20)$$

In Fig. 3 $|p_{\rm edge}/\rho_0 c V_s|$ vs. ka is plotted (solid curve, using the last formula of Eq. (20)) for a Gaussian velocity profile $\exp(-\alpha(\sigma/a)^2)$, $\alpha=2$ and truncated at $\sigma=a$, approximated using three Zernike coefficients $u_0=1.0000$, $u_1=$ -0.9392, $u_2=0.3044$.

The case with $u_0=1$, $u_1=u_2=\cdots=0$ in Eqs. (19–20) yields the same result as Eq. (14) with $n=0$, as it should. Observe also that the real part in Eq. (20) has $O[(ka)^{2n+1}]$-behavior as $ka\to 0$. As a consequence of this and the fact that $u_0=1$ by definition, the coefficient of $(ka)^2$ in $p_{\rm edge}$ equals $\frac{1}{2}\rho_0 c V_s$ for any profile $v(\sigma)$.

The formulas on the last lines of Eqs. (14) and (20) can further be checked against one another, because

$$s^{(n)}(\sigma)=V_s\sum_{j=0}^{n}(-1)^j\frac{2j+1}{j+1}\frac{\binom{n}{j}}{\binom{n+j+1}{n}}(n+1)R^0_{2n}(\sigma/a)\,, \qquad (21)$$

see Ref.21, Eq. (10). For instance, when $n=1$, one has $s^{(1)}(\sigma)=V_s(R^0_0(\sigma/a)-R^0_2(\sigma/a))$, and one has to check that

$$\frac{\ell}{\Gamma^2(\frac{1}{2}\ell+2)}=\frac{1}{2}\Big[\frac{1}{\Gamma^2(\frac{1}{2}\ell+1)}-\frac{(-\frac{1}{2}\ell+1)^2}{\Gamma^2(\frac{1}{2}\ell+2)}\Big]\,, \qquad (22)$$

which indeed holds. Accordingly, Fig. 2 (and Figs. 4–6) could have been produced equally well within the framework of Zernike expansions.

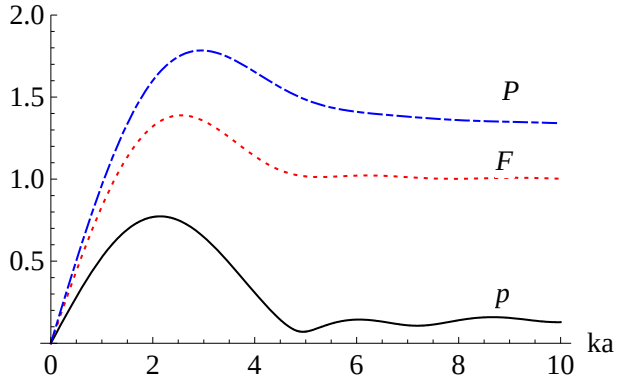

FIG. 3. (Color online) p: The pressure at the edge $|p_{\rm edge}/\rho_0 c V_s|$ vs. ka, (solid curve) using Eq. (20). F: the reaction force $|\frac{F}{\pi\rho_0 c V_s a^2}|$ vs. ka (dotted curve) using Eqs. (30) and (31). P: the power $|\frac{P}{\pi\rho_0 c V_s^2 a^2}|$ vs. ka (dash-dotted curve), using Eqs. (39) and (40). All curves for a truncated Gaussian velocity profile $\exp(-\alpha(\sigma/a)^2)$, $\alpha = 2$, approximated using three Zernike coefficients u_0 = 1.0000, u_1 = -0.9392, u_2 = 0.3044.

IV. REACTION ON RADIATOR

According to Eq. (3), the total reaction force F on the radiator is given by

$$F = \int_S p dS = \int_0^a \int_0^{2\pi} p((\sigma\cos\psi, \sigma\sin\psi, 0))\sigma d\sigma d\psi$$

$$= 2\pi \int_0^a i\rho_0 ck \int_0^\infty \frac{J_0(\sigma u)V(u)}{(u^2-k^2)^{1/2}} u du\, \sigma d\sigma \,. \qquad (23)$$

Because $\int_0^a J_0(\sigma u)\sigma d\sigma = a u^{-1} J_1(au)$, there results

$$F = 2\pi i \rho_0 cka \int_0^\infty \frac{J_1(au)V(u)}{(u^2-k^2)^{1/2}} du \,. \qquad (24)$$

A. Stenzel functions

With $v(\sigma) = s^{(n)}(\sigma)$ and its Hankel transform $V^{(n)}(u)$ given by Eqs. (6)–(7), the total reaction force $F^{(n)}$ on the radiator is given by

$$\frac{F^{(n)}}{\pi\rho_0 c V_s a^2} = (n+1)!\big(\frac{2}{a}\big)^{n+1} ika \int_0^\infty \frac{J_1(au)J_{n+1}(au)}{u^{n+1}(u^2-k^2)^{1/2}} du \,. \qquad (25)$$

The integral at the right-hand side of Eq. (25) has been evaluated in Appendix A.1, and the result is that

$$\begin{aligned}\frac{F^{(n)}}{\pi\rho_0 c V_s a^2} &= (n+1)!\big(\frac{2}{a}\big)^{n+1} ka\Big[\int_0^k \frac{J_1(au)J_{n+1}(au)}{u^{n+1}\sqrt{k^2-u^2}} du \\ &\quad + i\int_k^\infty \frac{J_1(au)J_{n+1}(au)}{u^{n+1}\sqrt{u^2-k^2}} du\Big] \\ &= (n+1)!\Big[\sum_{j=0}^\infty \frac{(-1)^j(2j+3)_n (ka)^{2j+2}}{\Gamma(n+j+2)\Gamma(n+j+3)} \\ &\quad + i\sum_{j=0}^\infty \frac{(-1)^j(2j+2)_n (ka)^{2j+1}}{\Gamma(n+j+3/2)\Gamma(n+j+5/2)}\Big] \\ &= -(n+1)!\sum_{\ell=1}^\infty \frac{(\ell+1)_n (-ika)^\ell}{\Gamma(n+\frac{1}{2}\ell+1)\Gamma(n+\frac{1}{2}\ell+2)} \,. \end{aligned} \qquad (26)$$

The middle expression for $F^{(n)}$ in Eq. (26) can be used to express $\Re F^{(n)}$ and $\Im F^{(n)}$ in terms of Bessel functions of the first kind and Struve functions, respectively. This yields

$$\frac{F^{(0)}}{\pi\rho_0 c V_s a^2} = 1 - \frac{J_1(2z)}{z} + i\frac{\mathbf{H_1}(2z)}{z} \,, \qquad (27)$$

$$\begin{aligned}\frac{F^{(1)}}{\pi\rho_0 c V_s a^2} &= 1 - \frac{6J_1(2z) - 4zJ_0(2z) - 2z}{z^3} \\ &\quad - i\frac{4z\mathbf{H_0}(2z) - 6\mathbf{H_1}(2z)}{z^3} \,, \end{aligned} \qquad (28)$$

$$\begin{aligned}\frac{F^{(2)}}{\pi\rho_0 c V_s a^2} &= 1 - 24\frac{(5-z^2)J_1(2z) - \frac{7}{2}zJ_0(2z) - \frac{3}{2}z}{z^5} \\ &\quad + 24i\frac{(5-z^2)\mathbf{H_1}(2z) - \frac{7}{2}z\mathbf{H_0}(2z) - \frac{2}{3\pi}z}{z^5} \,, \end{aligned} \qquad (29)$$

in which $z = ka$. This is in complete agreement with Ref.6, Eqs. (35), (40), (41), where it is recalled that Greenspan's V is equal to $\pi a^2 V_s$. Equation (27) is discussed in many texts, recently a simple and effective approximation of $\mathbf{H_1}(z)$ which is valid for all z is developed in Ref.29.

The expression for $F^{(n)}$ on the last line of Eq. (26) is in the form of a power series in $-ika$. In Ref.6, Eqs. (35a), (40b), (41b) the first few terms of the power series of $F^{(n)}$, $n = 0, 1, 2$, have been displayed. It turns out that this is in complete agreement with what Eq. (26) gives for these cases. Furthermore, it can be checked directly from Eq. (26) that the coefficient of $(ka)^2$ in $F^{(n)}$ equals $\frac{1}{2}\pi\rho_0 c V_s a^2$ (independently of n and in agreement with Greenspan's observation for $s^{(n)}$, $n = 0, 1, 2$). Thus $\Re[F^{(n)}] \approx \frac{1}{2}\pi\rho_0 c V_s a^2 (ka)^2$ for small ka. In Fig. 4 the force on the radiator $\frac{F^{(n)}}{\pi\rho_0 c V_s a^2}$ vs. ka is plotted (using the last formula of Eq. (26)) for the rigid piston ($n = 0$), the simply supported radiator ($n = 1$) and the first two clamped radiators ($n = 2, 3$).

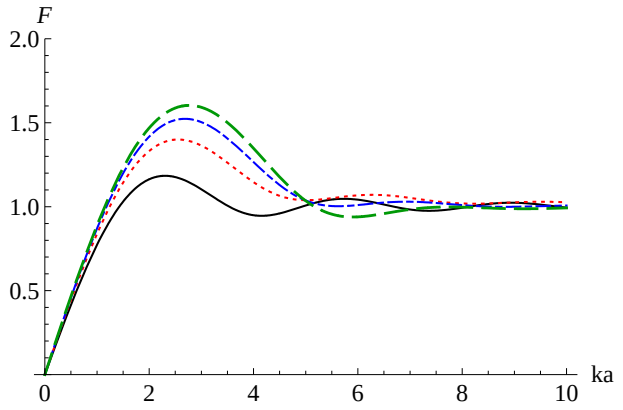

FIG. 4. (Color online) The force on the radiator $|\frac{F^{(n)}}{\pi\rho_0 c V_s a^2}|$ vs. ka, for the rigid piston ($n=0$) (solid curve), the simply supported radiator ($n=1$) (dotted curve) and the first two clamped radiators ($n=2,3$) (dash-dotted and dashed curves, respectively).

B. Zernike functions

With $v(\sigma)$ a linear combination of Zernike functions $R^0_{2n}(\sigma/a)$ as in Eq. (9) with Hankel transform $V(u)$ as given in Eq. (10), the total reaction force F is given by

$$\frac{F}{\pi\rho_0 c V_s a^2} = 2ik\sum_{n=0}^{\infty}(-1)^n u_n \int_0^\infty \frac{J_1(au)J_{2n+1}(au)}{u(u^2-k^2)^{1/2}}du\ . \tag{30}$$

The integrals at the right-hand side of Eq. (30) have been evaluated in Appendix A.2, with the result that

$$2ik\int_0^\infty \frac{J_1(au)J_{2n+1}(au)}{u(u^2-k^2)^{1/2}}du =$$

$$2k\int_0^k \frac{J_1(au)J_{2n+1}(au)}{u\sqrt{k^2-u^2}}du$$

$$+2ik\int_k^\infty \frac{J_1(au)J_{2n+1}(au)}{u\sqrt{u^2-k^2}^2}du$$

$$=\sum_{j=0}^{\infty}\frac{(-1)^j(j+1)_n(j+2)_n}{\Gamma(j+2n+2)\Gamma(j+2n+3)}(ka)^{2(n+j+1)}+$$

$$+i(-1)^n\sum_{j=0}^{\infty}\frac{(-1)^j(-j-\frac{1}{2})_n(-j+\frac{1}{2})_n}{\Gamma(j+n+3/2)\Gamma(j+n+5/2)}(ka)^{2j+1}$$

$$=-(-1)^n\sum_{\ell=1}^{\infty}\frac{(-\frac{1}{2}\ell)_n(-\frac{1}{2}\ell+1)_n}{\Gamma(\frac{1}{2}\ell+n+1)\Gamma(\frac{1}{2}\ell+n+2)}(-ika)^\ell\ . \tag{31}$$

In Fig. 3 $|\frac{F}{\pi\rho_0 c V_s a^2}|$ vs. ka is plotted (dotted curve, using the last formula of Eq. (31)) for the same Gaussian velocity profile as was considered in Subsec. III.B.

The case with $u_0=1$, $u_1=u_2=\cdots=0$, in Eq. (30)–(31) yields the same as Eq. (26) with $n=0$. The middle expression for F in Eq. (31) can be used to express $\Re F$ and $\Im F$ in terms of Bessel functions of the first kind and Struve functions, respectively. As with the Stenzel functions in Eqs. (27)–(29), this soon gets cumbersome. Finally, the single-series expressions on the last lines of Eqs. (26) and (31) can be checked against one another on basis of the Zernike representation in Eq. (21) of $s^{(n)}(\sigma)$, just as this was done with the two single-series expressions for $p_{\rm edge}$ in Sec. III.

Equation (31) shows that the real part has a non-zero coefficient for $(ka)^2$ only when $n=0$. Accordingly, the coefficient of $(ka)^2$ in F of Eq. (30) is equal to $\frac{1}{2}\pi\rho_0 c V_s a^2$ (because $u_0=1$ by definition), no matter what $v(\sigma)$ is. This is in agreement with the observation of Greenspan[6], Sec. IV, Eqs. (35a), (40b), (41b), that this holds for Stenzel functions $s^{(n)}$, $n=0,1,2$.

V. POWER OUTPUT AND DIRECTIVITY

The power is defined as the intensity pv^* integrated over the plane $z=0$. Thus, because v vanishes outside S,

$$P=\int_S p(\sigma)v^*(\sigma)dS\ , \tag{32}$$

where $p(\sigma)=p(\sigma\cos\psi,\sigma\sin\psi,0)$ is the pressure at an arbitrary point on S. According to Eq. (3) with $z=0$ and $w=\sigma$,

$$p(\sigma)=i\rho_0 ck\int_0^\infty \frac{V(u)}{(u^2-k^2)^{1/2}}J_0(\sigma u)udu\ ,\quad 0\le\sigma<\infty\ , \tag{33}$$

assumes the form of a Hankel transform, viz. of the function $i\rho_0 ckV(u)(u^2-k^2)^{-1/2}$, where $V(u)$ is the Hankel transform of $v(\sigma)$. By using Parseval's theorem for Hankel transforms in Eq. (32), it follows that

$$P=2\pi i\rho_0 ck\int_0^\infty \frac{V(u)V^*(u)}{(u^2-k^2)^{1/2}}udu\ . \tag{34}$$

A. Stenzel functions

With $v(\sigma)=s^{(n)}(\sigma)$ and $V(u)=S^{(n)}(u)$ as given by Eqs. (6)–(7), the power $P^{(n)}$ is given by

$$\frac{P^{(n)}}{\pi\rho_0 c V_s^2 a^2}=2\Big((n+1)!(\frac{2}{a})^n\Big)^2 k\int_0^\infty \frac{J^2_{n+1}(au)}{u^{2n+1}(u^2-k^2)^{1/2}}du\ . \tag{35}$$

The integral at the right-hand side of Eq. (35) has been evaluated in Appendix A.1, and the result is that

$$\frac{P^{(n)}}{\pi\rho_0 c V_s^2 a^2}=2\Big((n+1)!(\frac{2}{a})^n\Big)^2 k\Big[\int_0^k \frac{J^2_{n+1}(au)}{u^{2n+1}\sqrt{k^2-u^2}}du$$
$$+\,i\int_k^\infty \frac{J^2_{n+1}(au)}{u^{2n+1}\sqrt{u^2-k^2}}du\Big]$$

$$= \Big((n+1)!2^n\Big)^2 \Big[\sum_{j=0}^{\infty} \frac{(-1)^j (j+3/2)_n (ka)^{2j+2}}{\Gamma(n+j+2)\Gamma(2n+j+3)}$$

$$+ i \sum_{j=0}^{\infty} \frac{(-1)^j (j+1)_n (ka)^{2j+1}}{\Gamma(n+j+3/2)\Gamma(2n+j+5/2)}\Big]$$

$$= -((n+1)!2^n)^2 \sum_{\ell=1}^{\infty} \frac{(\frac{1}{2}(\ell+1))_n (-ika)^\ell}{\Gamma(n+\frac{1}{2}\ell+1)\Gamma(2n+\frac{1}{2}\ell+2)} \,. \tag{36}$$

The middle expression for $P^{(n)}$ in Eq. (36) can be used to express the real and imaginary part of $P^{(n)}$ in Bessel functions of the first kind and Struve functions, respectively. The case that $n = 0$ in Eq. (36) yields the same integral as the one that occurs in the expression of Eq. (25) for $F^{(n)}$ with $n = 0$, and so Eq. (27) can be used yielding

$$\frac{P^{(0)}}{\pi\rho_0 c V_s^2 a^2} = 1 - \frac{J_1(2z)}{z} + i\frac{\mathbf{H_1}(2z)}{z} \,. \tag{37}$$

For the cases $n = 1, 2$, Ref.6, Eqs. (45) and (47) express $P^{(n)}$ in terms of Bessel and Struve functions; these results have been checked against what Eq. (36) gives for $n = 1, 2$ and complete agreement has been observed. (This check has been carried out since, due to the very complicated nature of the resulting expressions, Greenspan had some doubts about correctness of his Eq. (47).)

The single-series expression on the last line of Eq. (36) has also been checked against Ref.6, Eqs. (45b) and (47b), where the first few terms are displayed: there is complete agreement. A further observation is that the coefficient of $(ka)^2$ in $P^{(n)}$ equals $\frac{1}{2}\pi\rho_0 c V_s^2 a^2$ (independent of n). Thus $\Re[P^{(n)}] \approx \frac{1}{2}\pi\rho_0 c V_s^2 a^2 (ka)^2$ for small ka. In Fig. 5 the real and imaginary parts of the power of the radiator $\frac{P^{(n)}}{\pi\rho_0 c V_s^2 a^2}$ vs. ka is plotted (using the last formula of Eq. (36)) for the rigid piston ($n = 0$), the simply supported radiator ($n = 1$) and the first two clamped radiators ($n = 2, 3$). Note that the power shown in Fig. 5 reaches a fixed value for large ka values. With the general approach developed in Subsec. V.B and D (in particular, Eqs. (39), (52) and (53)), it follows that these fixed values are given as

$$\lim_{ka\to\infty} \frac{P^{(n)}}{\pi\rho_0 c V_s^2 a^2} = 2\int_0^1 [(n+1)(1-\rho^2)^n]^2 \rho d\rho = \frac{(n+1)^2}{2n+1}. \tag{38}$$

However, for real sources like loudspeakers, the power will decay. This is because the velocity of the radiator will decrease for higher frequencies, in particular for loudspeakers above their resonance frequency.

B. Zernike functions

With $v(\sigma)$ a linear combination of Zernike functions $R_{2n}^0(\sigma/a)$ as in Eq. (9) with Hankel transform $V(u)$ as

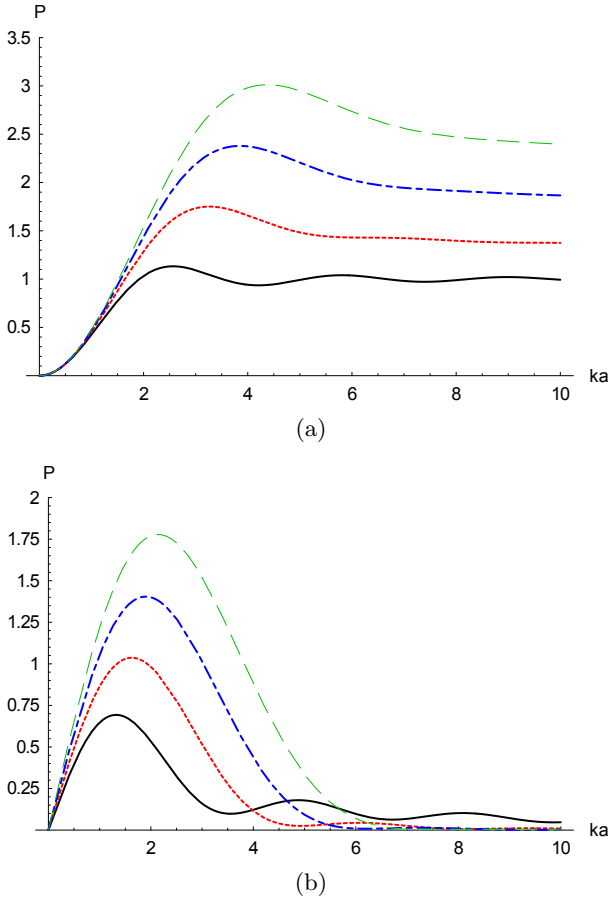

FIG. 5. (Color online) The power of the radiator $\frac{P^{(n)}}{\pi\rho_0 c V_s^2 a^2}$ vs. ka, for the rigid piston ($n = 0$) (solid curve), the simply supported radiator ($n = 1$) (dotted curve) and the first two clamped radiators ($n = 2, 3$) (dash-dotted and dashed curves, respectively). (a) Real part, (b) Imaginary part.

given in Eq. (10), the power P is given by

$$\frac{P}{\pi\rho_0 c V_s^2 a^2} = 2ik \sum_{n_1,n_2=0}^{\infty} (-1)^{n_1+n_2} u_{n_1} u_{n_2}^* \cdot \Big[\int_0^\infty \frac{J_{2n_1+1}(ua) J_{2n_2+1}(ua)}{u(u^2-k^2)^{1/2}} du\Big]. \tag{39}$$

The integrals at the right hand side of Eq. (39) have been evaluated in Appendix A.2, with the result that

$$2ik\int_0^\infty \frac{J_{2n_1+1}(ua)J_{2n_2+1}(ua)}{u(u^2-k^2)^{1/2}}du =$$

$$2k\int_0^k \frac{J_{2n_1+1}(ua)J_{2n_2+1}(ua)}{u\sqrt{k^2-u^2}}du +$$

$$2ik\int_k^\infty \frac{J_{2n_1+1}(ua)J_{2n_2+1}(ua)}{u\sqrt{u^2-k^2}}du =$$

$$\sum_{j=0}^{\infty} \frac{(-1)^j (j+1)_N (j+2n_2+2)_M}{\Gamma(j+2n_1+2)\Gamma(j+2N+3)} (ka)^{2(N+j+1)} +$$

$$i(-1)^M \sum_{j=0}^{\infty} \frac{(-1)^j(-j-1/2)_M(-j+1/2)_N}{\Gamma(j+M+3/2)\Gamma(j+N+5/2)}(ka)^{2j+1} =$$

$$-(-1)^M \sum_{\ell=1}^{\infty} \frac{(-\frac{1}{2}\ell)_M(-\frac{1}{2}\ell+1)_N(-ika)^\ell}{\Gamma(\frac{1}{2}\ell+M+1)\Gamma(\frac{1}{2}\ell+N+2)} , \qquad (40)$$

where $M = |n_1 - n_2|$ and $N = n_1 + n_2$.

The case with $u_0 = 1$, $u_1 = u_2 = \cdots = 0$ in Eqs. (39) and (40) yields the same as Eq. (36) with $n = 0$. The middle expression for the integral in Eq. (40) can be used to express real and imaginary parts in terms of Bessel functions of the first kind and Struve functions, respectively, but this gets out of hand quite soon. Finally, the single-series expressions in Eqs. (36) and (39)–(40) can be checked against one another using the Zernike expansion for $s^{(n)}$ in Eq. (21); this has been observed to give the same results for the case $s^{(1)}$. In Fig. 3 the normalized power $|\frac{P}{\pi\rho_0 c V_s^2 a^2}|$ (dash-dotted curve) is plotted using Eqs. (39) and (40) for a truncated Gaussian velocity profile $\exp(-\alpha(\sigma/a)^2)$, $\alpha = 2$, approximated using three Zernike coefficients u_0 =1.0000, u_1 =-0.9392, u_2=0.3044.

The series expansion in Eq. (40) shows that the coefficient of $(ka)^2$ is non-zero for $N = n_1 + n_2 = 0$ only (this is so since $(0)_N \neq 0$ for $N = 0$ only). Since by definition $u_0 = 1$, this shows that the coefficient of $(ka)^2$ in P in Eq. (39) is equal to $\frac{1}{2}\rho_0 c\pi V_s^2 a^2$, no matter what $v(\sigma)$ is.

C. Power evaluated from the far field

Usually one calculates the power of the radiator from p and v values at the radiator itself, but due to the conservation of energy the power can also be computed from sound field values at any distance from the radiator. Below it is shown that the power can be calculated in the far field with the techniques described in the preceding sections. The power as defined in Eq. (32) should be equal to the integral of pv^* over any surface $\sum$ in $z \geq 0$ containing the disk $\sigma \leq a$. Here v and p are related to one another in $z \geq 0$ according to

$$v = \frac{-1}{ik\rho_0 c}\frac{\partial p}{\partial \underline{n}} , \quad \underline{n} \text{ normal to } \Sigma . \qquad (41)$$

The imaginary part of P, the wattless component, manifests itself only close to the radiator and has no physical significance in the far field; it is thus customary to consider the real part of P only, especially when the non-rigid part of Σ in $z > 0$ is in the far field. It is shown by Bouwkamp[12] that

$$\Re[\int_\Sigma pv^* d\Sigma] = \frac{1}{2}\int_\Sigma (pv^* + p^*v) d\Sigma = 0 . \qquad (42)$$

Thus, taking for Σ the surface S_R of the hemisphere $x^2 + y^2 + z^2 \leq R^2$, $z \geq 0$ with $R \geq a$, together with the disk $x^2 + y^2 \leq R^2$, $z = 0$, one finds that

$$\Re[\int_S pv^* dS] = \Re[\int_{S_R} pv^* dS_R] . \qquad (43)$$

The right-hand side of Eq. (43) will now be considered when $R \to \infty$. According to Blackstock[1] it holds in the far field that

$$p = O(1/r), \; v = (\rho_0 c)^{-1} p(1 + O(1/r)) . \qquad (44)$$

Hence,

$$\Re[\int_{S_R} pv^* dS_R] = (\rho_0 c)^{-1} \int_{S_R} |p|^2 dS_R + O(R^{-1}) . \qquad (45)$$

From the Rayleigh representation of p in Eq. (1), it follows with the usual approximation arguments that

$$\begin{aligned} p(\underline{r}) &\approx i\rho_0 ck \frac{e^{-ikr}}{r} \int_0^a v(\sigma) J_0(k\sigma \sin\theta) \sigma d\sigma \\ &= i\rho_0 ck \frac{e^{-ikr}}{r} V(k \sin\theta) \end{aligned} \qquad (46)$$

with V the Hankel transform of v as before. Then taking spherical coordinates in the integral at the right-hand side of Eq. (45) and letting $R \to \infty$, it follows that

$$\Re[\int_{S_R} pv^* dS] = 2\pi\rho_0 ck^2 \int_0^{\pi/2} |V(k\sin\theta)|^2 \sin\theta d\theta . \qquad (47)$$

By changing integration variables in the integral at the right-hand side of Eq. (47) according to $u = k\sin\theta$, $0 \leq u \leq k$, the final result becomes

$$\Re[\int_{S_R} pv^* dS] = 2\pi\rho_0 ck \int_0^k \frac{|V(u)|^2}{\sqrt{k^2 - u^2}} u du . \qquad (48)$$

Compare Eq. (34).

D. Directivity

From the far-field expression in Eq. (46) for $p(\underline{r})$, $\underline{r} = (r\cos\psi\sin\theta, r\sin\psi\sin\theta, r\cos\theta)$, there results the directivity

$$\begin{aligned} D &= \frac{4\pi|V(0)|^2}{\int_0^{2\pi}\int_0^{\pi/2} |V(k\sin\theta)|^2 \sin\theta d\psi d\theta} \\ &= \frac{2|V(0)|^2}{\int_0^{\pi/2} |V(k\sin\theta)|^2 \sin\theta d\theta} , \end{aligned} \qquad (49)$$

see Kinsler et al.[2], Sec.8.9. This gives rise to the same integral as in Eq. (47). By Eqs. (2) and (5) it holds that $V(0) = \frac{1}{2}a^2 V_s$, and by Eq. (34) it holds that

$$\int_0^{\pi/2} |V(k\sin\theta)|^2 \sin\theta d\theta = \frac{1}{2\pi\rho_0 ck^2}\Re[P] . \qquad (50)$$

In Fig. 6 the directivity index ($DI = 10\log_{10} D$) vs. ka is plotted (using the last formula of Eq. (36) and Eqs. (49) and (50)) for the rigid piston ($n = 0$), the simply supported radiator ($n = 1$) and the first two clamped radiators ($n = 2, 3$).

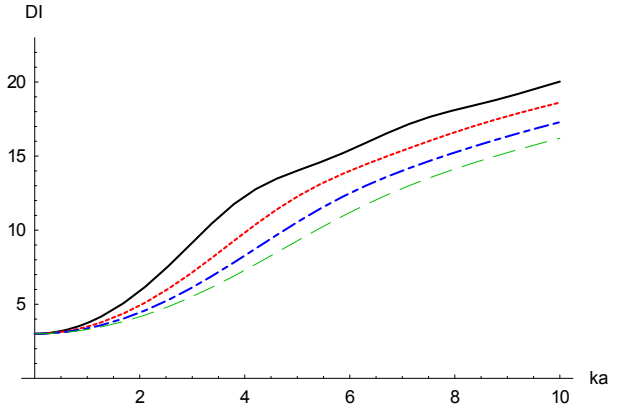

FIG. 6. (Color online) The directivity index $DI = 10\log_{10} D$ [dB] vs. ka, for the rigid piston ($n = 0$) (solid curve), the simply supported radiator ($n = 1$) (dotted curve) and the first two clamped radiators ($n = 2, 3$) (dash-dotted and dashed curves, respectively).

Consider the case that $ka \to 0$. By the observation at the end of Subsecs. V.A and B, it holds that $\Re[P] \approx \frac{1}{2}\pi\rho_0 c V_s^2 a^2 (ka)^2$. Therefore, as $ka \to 0$

$$D \approx \frac{2(\frac{1}{2}a^2 V_s)^2}{\frac{1}{2\pi\rho_0 ck^2}\frac{1}{2}\pi\rho_0 c V_s^2 a^2 (ka)^2} = 2\,, \tag{51}$$

or 3 dB, which is the same for a rigid piston[2] or a hemispherical source on an infinite baffle and is supported by Fig. 6.

Next consider the case that $ka \to \infty$, in the general setting of Subsec. V.B. Now, by Ref.22, 11.4.6,

$$\begin{aligned} &\int_0^k \frac{J_{2n_1+1}(ua)J_{2n_2+1}(ua)}{u\sqrt{k^2-u^2}}du = \\ &a\int_0^{ka} \frac{J_{2n_1+1}(v)J_{2n_2+1}(v)}{v\sqrt{(ka)^2-v^2}}dv \approx \\ &\frac{a}{ka}\int_0^\infty \frac{J_{2n_1+1}(v)J_{2n_2+1}(v)}{v}dv = \frac{1}{k}\frac{\delta n_1 n_2}{2(2n_1+1)}\,. \end{aligned} \tag{52}$$

Thus from Eq. (39)

$$\begin{aligned} \Re[P] &\approx 2\pi\rho_0 c V_s^2 a^2 \sum_{n=0}^\infty \frac{|u_n|^2}{2(2n+1)} \\ &= 2\pi\rho_0 c a^2 \int_0^1 |v(a\rho)|^2 \rho d\rho\,, \end{aligned} \tag{53}$$

where Parseval's theorem for Zernike expansions $v(\sigma) = V_s\sum_{n=0}^\infty u_n R_{2n}^0(\sigma/a)$ has been used. It thus follows that, as $ka \to \infty$,

$$\begin{aligned} D &\approx \frac{2(\frac{1}{2}a^2 V_s)^2}{\frac{1}{2\pi\rho_0 ck^2}2\pi\rho_0 c a^2 \int_0^1 |v(a\rho)|^2\rho d\rho} \\ &= \frac{\frac{1}{2}(ka)^2 V_s^2}{\int_0^1 |v(a\rho)|^2\rho d\rho}\,. \end{aligned} \tag{54}$$

In case that $v = s^{(n)}$, the last member of Eq. (54) is given by $(2n+1)(n+1)^{-1}(ka)^2$; in Kinsler et al.[2], end of Subsec. 8.9. this result for the case $n = 0$ is given.

VI. ESTIMATING POWER FROM NEAR-FIELD ON-AXIS MEASUREMENTS

In Aarts and Janssen[21] a method has been introduced recently to estimate a radially symmetric velocity profile $v(\sigma)$, $0 \le \sigma \le a$, from on-axis sound pressure data, in terms of Zernike expansion coefficients. The basis of this method is the explicit formula , see Ref.21, Eq. (17),

$$p((0,0,r)) = \frac{1}{2}\rho_0 c V_s (ka)^2 \sum_{n=0}^\infty \gamma_n(k,r)u_n \tag{55}$$

for the on-axis pressure, where the $\gamma_n(k,r)$ are explicitly given in terms of spherical Bessel and Hankel functions. The formulas in Subsec. V.B then show how these estimated coefficients give rise to a means to compute the power and directivity.

VII. CONCLUSIONS

Greenspan's results[6] on acoustic quantities related to the pressure due to a velocity profile on a piston radiator in an infinite baffle are treated in a unified way. By expanding the velocity profile in terms of Zernike functions, the pressure at the edge of a radiator, the reaction force on the radiator, the power output and directivity of the radiator can be expressed in an attractive way as power series in ka. Since many velocity profiles have a representation in terms of Zernike functions with explicitly computable coefficients, the results of this paper constitute a considerable generalization of Greenspan's results.

APPENDIX A: EVALUATION OF BESSEL INTEGRALS

In this appendix the integrals

$$i\int_0^\infty \frac{J_{m+1}(au)J_{n+1}(au)}{u^{n+m+1}(u^2-k^2)^{1/2}}du \tag{A1}$$

are evaluated. These integrals occur in relation to the pressure at the edge ($m = -1$), the reaction on the radiator ($m = 0$), and the power if the velocity profile $v(\sigma)$ is a Stenzel function $s^{(n)}(\sigma)$ or a linear combination of Stenzel functions. Furthermore, the integrals

$$i\int_0^\infty \frac{J_m(au)J_{n+1}(au)}{(u^2-k^2)^{1/2}}du\,, \tag{A2}$$

$$i\int_0^\infty \frac{J_{m+1}(au)J_{n+1}(au)}{u(u^2-k^2)^{1/2}}du\,, \tag{A3}$$

with integer $n, m \ge 0$ such that $n - m$ even and ≥ 0 are evaluated. These integrals occur in connection with the pressure at the edge ($m = 0$ in Eq. (A2)), reaction on the radiator ($m = 0$ in Eq. (A3)), and the power (general m, n in Eq. (A3)) if the velocity profile is a linear combination of Zernike functions.

The integrals are evaluated in the form $\Re + i\Im$, where $\Re$ and $\Im$ arises from the integration ranges $[0,k]$ and $[k,\infty)$, respectively. These $\Re$ and $i\Im$ parts are given as power series in ka in a form from which the close relationship with Bessel functions of the first kind,

$$J_\nu(x) = (\frac{1}{2}x)^\nu \sum_{j=0}^{\infty} \frac{(-\frac{1}{4}x^2)^j}{\Gamma(j+1)\Gamma(j+\nu+1)} , \qquad \text{(A4)}$$

and Struve functions

$$\mathbf{H}_\nu(x) = (\frac{1}{2}x)^{\nu+1} \sum_{j=0}^{\infty} \frac{(-\frac{1}{4}x^2)^j}{\Gamma(j+\frac{3}{2})\Gamma(j+\nu+\frac{3}{2})} , \qquad \text{(A5)}$$

is apparent. Furthermore, the two series for $\Re$ and $i\Im$ are reorganized and combined into a concise single power series in $-ika$ for the various integrals.

A formula, in terms of hypergeometric functions ${}_3F_4$ of the integrals

$$(\int_0^k + \int_k^\infty) u^{\alpha-1}(u^2-k^2)^{\beta-1} J_\mu(au) J_\nu(au) du \qquad \text{(A6)}$$

can be found in Prudnikov et al.[30], § 2.12.32, items 3 and 8. These formulas are quite complicated, there is no indication of where a proof can be found, several degenerations and simplifications occur due to special values of α, β, μ, ν to which Eqs. (A1)–(A3) restrict, and no attention is paid to bringing the results into an attractive form. The results obtained here have been checked against the results in Prudnikov et al. for the special values of α, β, μ, ν that occur here. The method of the proofs used is taken from Watson[31], Sec. 13.6.

1. Evaluation of Eq. (A1)

Let $n, m = 0, 1, \cdots$. The case where $m = -1$ in Eq. (A1) is dealt with at the end of this section. It holds that

$$i\int_0^\infty \frac{J_{n+1}(au)J_{m+1}(au)}{u^{n+m+1}(u^2-k^2)^{1/2}} du$$

$$= \int_0^k \frac{J_{n+1}(au)J_{m+1}(au)}{u^{n+m+1}\sqrt{k^2-u^2}} du +$$

$$i\int_k^\infty \frac{J_{n+1}(au)J_{m+1}(au)}{u^{n+m+1}\sqrt{u^2-k^2}} du . \qquad \text{(A7)}$$

There is the integral representation, see Watson[31], Sec. 13.6,

$$J_\mu(au)J_\nu(au) =$$

$$\frac{1}{2\pi i}\int_{-\infty i}^{\infty i} \frac{\Gamma(-s)\Gamma(\mu+\nu+2s+1)(\frac{1}{2}au)^{\mu+\nu+2s}}{\Gamma(\mu+s+1)\Gamma(\nu+s+1)\Gamma(\mu+\nu+s+1)} ds , \qquad \text{(A8)}$$

where the integration contour has the poles of $\Gamma(-s)$ on its right and those of $\Gamma(\mu+\nu+2s+1)$ on its left (thus $-\frac{1}{2}(\mu+\nu+1) < \Re(s) < 0$).

For the first integral in Eq. (A7), second line, the result of Eq. (A8) is used together with

$$\int_0^k \frac{u^\alpha}{\sqrt{k^2-u^2}} du = \frac{1}{2}k^\alpha \frac{\Gamma(\frac{1}{2})\Gamma(\frac{1}{2}\alpha+\frac{1}{2})}{\Gamma(\frac{1}{2}\alpha+1)} , \ \Re(\alpha) > -1 . \qquad \text{(A9)}$$

This yields

$$\int_0^k \frac{J_{n+1}(au)J_{m+1}(au)}{u^{n+m+1}\sqrt{k^2-u^2}} du = \frac{1}{2}\Gamma(\frac{1}{2})(\frac{1}{2}a)^{n+m+1}\frac{1}{2\pi i}\cdot \int_{-\infty i}^{\infty i} \frac{\Gamma(-s)\Gamma(n+m+2s+3)(\frac{1}{2}ka)^{2s+1}}{\Gamma(n+s+2)\Gamma(m+s+2)\Gamma(n+m+s+3)}\cdot \frac{\Gamma(s+1)}{\Gamma(s+\frac{3}{2})} ds , \qquad \text{(A10)}$$

where the two occurring integrals have been interchanged. The integration in Eq. (A10) is closed to the right, thereby enclosing all poles of $\Gamma(-s)$ at $s = j$ with residues $(-1)^{j+1}/j!$, and it follows from Cauchy's theorem that

$$\int_0^k \frac{J_{n+1}(au)J_{m+1}(au)}{u^{n+m+1}\sqrt{k^2-u^2}} du = \frac{1}{2}\Gamma(\frac{1}{2})(\frac{1}{2}a)^{n+m+1}\cdot \sum_{j=0}^{\infty} \frac{\Gamma(2j+n+m+3)}{\Gamma(j+m+2)\Gamma(j+3/2)}\cdot \frac{(-1)^j(\frac{1}{2}ka)^{2j+1}}{\Gamma(j+n+2)\Gamma(j+n+m+3)} . \qquad \text{(A11)}$$

Now assume that $n \geq m$. Then it holds that

$$\frac{\Gamma(n+m+2j+3)}{\Gamma(m+j+2)\Gamma(j+3/2)} = \frac{2^{2m+2j+2}}{\Gamma(\frac{1}{2})}(2m+2j+3)_{n-m}(j+\frac{3}{2})_m , \qquad \text{(A12)}$$

where Pochhammer's symbol $(x)_\ell$ has been used,

$$(x)_\ell = \frac{\Gamma(x+\ell)}{\Gamma(x)} ; \ (x)_0 = 1 , \quad (x)_\ell = x(x+1)\cdot\ldots\cdot(x+\ell-1), \ \ell = 1, 2, \cdots . \qquad \text{(A13)}$$

Therefore,

$$\int_0^k \frac{J_{n+1}(au)J_{m+1}(au)}{u^{n+m+1}\sqrt{k^2-u^2}} du = 2^{m-n-1}a^{n+m+1} \cdot \sum_{j=0}^{\infty} \frac{(-1)^j(2m+2j+3)_{n-m}(j+3/2)_m}{\Gamma(j+n+2)\Gamma(j+n+m+3)}(ka)^{2j+1} . \qquad \text{(A14)}$$

Next, for the second integral on the second line of Eq. (A7), the plan of the proof is the same, except that now

$$\int_k^\infty \frac{u^\alpha}{\sqrt{u^2-k^2}} du = \frac{1}{2}k^\alpha \frac{\Gamma(\frac{1}{2})\Gamma(-\frac{1}{2}\alpha)}{\Gamma(\frac{1}{2}-\frac{1}{2}\alpha)} , \ \Re(\alpha) < 0 , \qquad \text{(A15)}$$

is used. This yields the same expression as in Eq. (A10), except that the $\Gamma(s+1)/\Gamma(s+3/2)$ just in front of ds has to be replaced by $\Gamma(-s-1/2)/\Gamma(-s)$, thereby canceling the $\Gamma(-s)$ just behind the integral sign. Now the poles of $\Gamma(-s-1/2)$ at the points $s = j-1/2$ have to be taken into account, and this yields (using Eq. (A12) with $j-1/2$ instead of j)

$$\int_k^\infty \frac{J_{n+1}(au)J_{m+1}(au)}{u^{n+m+1}\sqrt{u^2-k^2}}du = 2^{m-n-1}a^{n+m+1}\ .$$
$$\sum_{j=0}^\infty \frac{(-1)^j(2j+2m+2)_{n-m}(j+1)_m}{\Gamma(j+n+3/2)\Gamma(j+n+m+5/2)}(ka)^{2j}\ . \tag{A16}$$

This yields a power series for the real part in Eq. (A7) per Eq. (A14) and the imaginary part in Eq. (A7) per Eq. (A16) that shows a close relationship with the Bessel and Struve functions in Eq. (A4) and (A5), respectively. It is actually possible to express the results of Eqs. (A14) and (A16) systematically in terms of Bessel and Struve functions by manipulating the polynomial of degree n in j occurring in the numerator of the coefficients in the series in Eqs. (A14) and (A16).

The case that $m = -1$ can be dealt with in a completely similar fashion, except that in Eq. (A12) the definition $(x)_{-1} = (x-1)^{-1}$ of Pochhammer's symbol with subscript $\ell = -1$ should be used (this is consistent with the Γ-function based definition in Eq. (A13)). With some further rewriting this then yields the identity of the quantities in the second and third member between [ ] in Eq. (14) in the main text.

A single power series in $-ika$ for Eq. (A7) follows on combining Eqs. (A14) and (A16). Doing the administration with the $(-1)^j = (-i)^{2j}$, there results

$$i\int_0^\infty \frac{J_{n+1}(au)J_{m+1}(au)}{u^{n+m+1}(u^2-k^2)^{1/2}}du = -\frac{1}{k}2^{m-n-1}a^{n+m}\ .$$
$$\sum_{\ell=1}^\infty \frac{(\ell+2m+1)_{n-m}(\frac{1}{2}(\ell+1))_m}{\Gamma(\frac{1}{2}\ell+n+1)\Gamma(\frac{1}{2}\ell+n+m+2)}(-ika)^\ell\ . \tag{A17}$$

2. Evaluation of Eqs. (A2) and (A3)

Let n, m be integers ≥ 0 with $n-m$ even and ≥ 0. The proof for the integral in Eq. (A2) follows the same reasoning as for the integral in Eq. (A1). Letting

$$p = \frac{n-m}{2}\ ,\quad q = \frac{n+m}{2}\ , \tag{A18}$$

it is found without any particular problem that

$$\int_0^k \frac{J_{n+1}(au)J_m(au)}{\sqrt{k^2-u^2}}du =$$
$$\frac{1}{2}\sum_{j=0}^\infty \frac{(-1)^j(j+1)_q\,(j+m+1)_p(ka)^{2(j+q)+1}}{\Gamma(n+j+2)\Gamma(j+2q+2)}\ . \tag{A19}$$

For the integration range $[k,\infty)$ in the integral in Eq. (A2), the method based on Eqs. (A8) and (A15) yields an expression as in the second member of Eq. (A10), except that the $\Gamma(s+1)/\Gamma(s+3/2)$ appearing in front of ds should be replaced by $\Gamma(-s-q-1/2)/\Gamma(-s+q)$, thereby canceling all poles of the $\Gamma(-s)$ appearing just behind the integral sign in Eq. (A10). It is then found upon some further administration with Γ-functions that

$$\int_k^\infty \frac{J_{n+1}(au)J_m(au)}{\sqrt{u^2-k^2}}du =$$
$$\frac{1}{2}\sum_{k=0}^\infty \frac{(-1)^{j+p}(-j+1/2)_q\,(-j+1/2)_p}{\Gamma(j+p+3/2)\Gamma(j+q+3/2)}\,(ka)^{2j}\ . \tag{A20}$$

From Eqs. (A19) and (A20) a single series expression for Eq. (A2) can be derived. To this end, the summation index j in Eq. (A19) is changed into $j-q-1$ with $j = q+1, q+2, \cdots$. Next, it is observed that $n-q=p$, $m-q=-p$, and that

$$(j-q)_q = (-1)^q(-j+1)_q\,,\ (j-p)_p = (-1)^p(-j+1)_p\ . \tag{A21}$$

As a consequence of $(-j+1)_q = 0$ for $j = 1, \cdots, q$ it follows that the new summation index j can be taken to range from 1 to ∞. This all yields the result

$$\int_0^k \frac{J_{n+1}(au)J_m(au)}{\sqrt{k^2-u^2}}du =$$
$$-\frac{(-1)^p}{2ka}\sum_{j=1}^\infty \frac{(-1)^j(-j+1)_p\,(-j+1)_q(ka)^{2j}}{\Gamma(j+p+1)\Gamma(j+q+1)}\ . \tag{A22}$$

Then combining Eq. (A20) and Eq. (A22) while administrating the $(-1)^j = (-i)^{2j}$, yields the single-series expression

$$i\int_0^\infty \frac{J_{n+1}(au)J_m(au)}{(u^2-k^2)^{1/2}}du =$$
$$-\frac{(-1)^p}{2ka}\sum_{\ell=1}^\infty \frac{(-\frac{1}{2}\ell+1)_p\,(-\frac{1}{2}\ell+1)_q}{\Gamma(\frac{1}{2}\ell+p+1)\Gamma(\frac{1}{2}\ell+q+1)}(-ika)^\ell\ . \tag{A23}$$

The treatment of the integral in Eq. (A3) is entirely similar. There results

$$i\int_0^\infty \frac{J_{n+1}(au)J_{m+1}(au)}{u(u^2-k^2)^{1/2}}du = \int_0^k \frac{J_{n+1}(au)J_{m+1}(au)}{u\sqrt{k^2-u^2}}du$$
$$+\,i\int_k^\infty \frac{J_{n+1}(au)J_{m+1}(au)}{u\sqrt{u^2-k^2}}du =$$
$$\frac{1}{2k}\sum_{j=0}^\infty \frac{(-1)^j(j+1)_q\,(j+m+1)_p}{\Gamma(j+n+2)\Gamma(j+2q+3)}(ka)^{2(q+1+j)} +$$
$$\frac{1}{2}ia(-1)^p\sum_{j=0}^\infty \frac{(-1)^j(-j-1/2)_p\,(-j+1/2)_q}{\Gamma(j+p+3/2)\Gamma(j+q+5/2)}(ka)^{2j} =$$
$$-\frac{(-1)^p}{2k}\sum_{\ell=1}^\infty \frac{(-\frac{1}{2}\ell)_p(-\frac{1}{2}\ell+1)_q}{\Gamma(\frac{1}{2}\ell+p+1)\Gamma(\frac{1}{2}\ell+q+2)}(-ika)^\ell\ . \tag{A24}$$

Here n and m are integers ≥ 0 with $n-m$ even and ≥ 0, and p and q given by Eq. (A18).

The results for the integrals in Eqs. (A2) and (A3) just given, have been checked by using[22] $z^{-1}J_{m+1}(z) = (2(m+1))^{-1}(J_m(z)+J_{m+2}(z))$ in Eq. (A3).

APPENDIX B: CONVERGENCE ANALYSIS OF THE SERIES

The series in Eqs. (14), (26), (36) for the case of Stenzel functions on one hand and those in Eqs. (20), (31), (40) for the case of Zernike functions on the other, are all of a very similar nature with regard to convergence and accuracy matters. It therefore suffices to consider only the series in Eq. (14) and the series in Eq. (20). Next, from a simple comparison of the coefficients in the two series

$$\sum_{\ell=1}^{\infty} \frac{(\ell)_n\, z^\ell}{\Gamma^2(n+\frac{1}{2}\ell+1)} \quad \text{and} \quad \sum_{\ell=1}^{\infty} \Big(\frac{(-\frac{1}{2}\ell+1)_n}{\Gamma(n+\frac{1}{2}\ell+1)}\Big)^2 z^\ell \,, \tag{B1}$$

it is seen that for either series $n=0$ is worst case. The series to be considered becomes for either case

$$S(z=-ika) = \sum_{\ell=1}^{\infty} \frac{z^\ell}{\Gamma^2(\frac{1}{2}\ell+1)} \,. \tag{B2}$$

From Stirling's formula $\Gamma(x+1) \approx \mathrm{e}^{-x}x^{x+1/2}\sqrt{2\pi}$ it readily follows that the modulus of the terms t_ℓ in the series in Eq. (B2) is accurately estimated by

$$|t_\ell| \approx m_\ell = \frac{1}{\pi\ell}\Big(\frac{2\mathrm{e}|z|}{\ell}\Big)^\ell \,. \tag{B3}$$

Hence, m_ℓ is of order unity and less from $\ell = 2\mathrm{e}|z|$ onwards. Next, setting $\ell = 2\mathrm{e}|z|+b$ with $0 \leq b \leq \ell$, it follows that

$$m_\ell = \frac{1}{\pi\ell}(1-\frac{b}{\ell})^\ell \leq \frac{1}{\pi\ell}\mathrm{e}^{-b} = \frac{1}{\pi\ell}\mathrm{e}^{2\mathrm{e}|z|-\ell} \,. \tag{B4}$$

Hence, for integer $L \geq 2\mathrm{e}|z|$ it holds that

$$\sum_{\ell=L}^{\infty} m_\ell \leq \frac{\mathrm{e}^{2\mathrm{e}|z|-L}}{\pi L(\mathrm{e}-1)} \,. \tag{B5}$$

When, for instance, $L \geq 2\mathrm{e}|z|+10$, the absolute accuracy by including in the series in Eq. (B2) the terms with $\ell = 1, \cdots, L-1$ is at least 10^{-6}. Note that the true value of $S(z=-ika)$ is of order unity, see Fig. 2. However, loss-of-digits occurs in summing the series. The maximum value over $\ell = 1, 2, \cdots$ of m_ℓ in Eq. (B3) is assumed near $2|z|$ and is accurately given by $\mathrm{e}^{2|z|}/2\pi|z|$. For instance, when $|z| \leq 12$ (which is the case in all figures) this maximum is $\leq 3.5\,10^8$. As a result, when machine precision is 10^{-15}, an absolute accuracy of 10^{-6} is obtained in all cases when $0 \leq ka \leq 12$ assuming that the series is truncated at an integer $L \geq 2\mathrm{e}ka+10$.

[1] D.T. Blackstock. *Fundamentals of Physical Acoustics.* John Wiley & Sons, New York, 2000.

[2] L.E. Kinsler, A.R. Frey, A.B. Coppens, and J.V. Sanders. *Fundamentals of Acoustics.* John Wiley & Sons, New York, 1982.

[3] P.M. Morse and K.U. Ingard. *Theoretical Acoustics.* McGraw-Hill Book Company, New York, 1968.

[4] A.D. Pierce. *Acoustics, An Introduction to Its Physical Principles and Applications.* Acoustical Society of America through the American Institue of Physics, 1989.

[5] H. Stenzel and O. Brosze. *Guide to computation of sound phenomena (published in German as Leitfaden zur Berechnung von Schallvorgängen), 2nd ed.* Springer-Verlag, Berlin, 1958.

[6] M. Greenspan. Piston radiator: Some extensions of the theory. *J. Acoust. Soc. Am.*, 65(3):608–621, March 1979.

[7] G.R. Harris. Review of transient field theory for a baffled planar piston. *J. Acoust. Soc. Am.*, 70:10–20, 1981.

[8] H. Stenzel. On the acoustical radiation of membranes (published in German as Über die akustische Strahlung von Membranen). *Ann. Physik*, 7:947–982, 1930.

[9] L.V. King. On the acoustic radiation field of the piezoelectric oscillator and the effect of viscosity on transmission. *Can. J. Res.*, 11:135–155, 1934.

[10] A. Schoch. Contemplations on the sound field of piston membranes (published in German as Betrachtungen über das Schallfeld einer Kolbenmembran). Akust. Z. 6, 318-326 (1941).

[11] J. A. Archer-Hall, A. I. Bashter, and A. J. Hazelwood. A means for computing the Kirchhoff surface integral for a disk radiator as a single integral with fixed limits. *J. Acoust. Soc. Am.*, 65(6):1568-1570, 1979.

[12] C.J. Bouwkamp. A contribution to the theory of acoustic radiation. *Philips Research Reports, Eindhoven, The Netherlands*, 1:251–277, 1946.

[13] F. Oberhettinger. On transient solutions of the "baffled piston" problem. *J. of Research of the Nat. Bureau of Standards-B, Mathematics and Mathematical Physics*, 65B(1):1–6, Jan.–March 1961.

[14] T. Hansen. Probe-corrected near-field measurements on a truncated cylinder. *J. Acoust. Soc. Am.*, 119:792–807, 2006.

[15] D.A. Hutchins, H.D. Mair, P.A. Puhach, and A.J. Osei. Continuous-wave pressure fields of ultrasonic transducers. *J. Acoust. Soc. Am.*, 80(1):1–12, July 1986.

[16] R.J. McGough, T.V. Samulski, and J.F. Kelly. An efficient grid sectoring method for calculations of the near field pressure generated by a circular piston. *J. Acoust. Soc. Am.*, 115:1942–1954, 2004.

[17] J.F. Kelly and R.J. McGough. An annular superposition integral for axisymmetric radiators. *J. Acoust. Soc. Am.*, 121(2):759–765, February 2007.

[18] T.D. Mast and F. Yu. Simplified expansions for radiation from a baffled circular piston. *J. Acoust. Soc. Am.*, 118(6):3457–3464, December 2005.

[19] T. Mellow. On the sound field of a resilient disk in an infinite baffle. *J. Acoust. Soc. Am.*, 120(1):90–101, July 2006.

[20] R. C. Wittmann and A. D. Yaghjian. Spherical-wave expansions of piston-radiator fields. *J. Acoust. Soc. Am.*, 90(3):1647–1655, September 1991.

[21] R.M. Aarts and A.J.E.M. Janssen. On-axis and far-field sound radiation from resilient flat and dome-shaped radiators. *J. Acoust. Soc. Am.*, 125(3):1444-1455, March 2009.

[22] M. Abramowitz and I.A. Stegun. *Handbook of Mathematical Functions.* Dover, New York, 1972.

[23] T. Hasegawa, N. Inoue, and K. Matsuzawa. A new rigorous expansion for the velocity potential of a circular piston

source. *J. Acoust. Soc. Am.*, 74(3):1044–1047, September 1983.

[24] N.W. McLachlan. The acoustic and inertia pressure at any point on a vibrating circular disk. *Philosophical Magazine and Journal of Science*, 14 (7th series):1012–1025, 1932.

[25] F. Zernike. Diffraction theory of the knife-edge test and its improved version, the phase-contrast method (published in German as Beugungstheorie des Schneidenverfahrens und seiner verbesserten Form, der Phasenkontrastmethode). *Physica* 1:689-704, 1934.

[26] J.W.S. Rayleigh. *The Theory of Sound, Vol. 2.* Dover, New York, (reprinted 1945), 1896.

[27] B.R.A. Nijboer. *The Diffraction Theory of Aberrations.* Ph.D. dissertation, University of Groningen, The Netherlands, 1942.

[28] A.G. Warren. A note on the acoustic pressure and velocity relations on a circular disc and in a circular orifice. *Proc. Phys. Soc. (London)*, 40:296–299, June 1928.

[29] R.M. Aarts and A.J.E.M. Janssen. Approximation of the Struve function $\mathbf{H}_1(z)$ occurring in impedance calculations. *J. Acoust. Soc. Am.*, 113(5):2635-2637, May 2003.

[30] A.P. Prudnikov, Yu.A. Brychkov, and O.I. Marichev, *Integrals and Series, Volume 2: Special Functions* (Gordon and Breach Science, New York, 1986).

[31] G.N. Watson, *A Treatise on the Theory of Bessel Functions* (Cambridge University Press, Cambridge, 1944).